https://doi.org/10.5194/gmd-2024-193
Preprint. Discussion started: 3 December 2024

Geoscientific Model Development Discussions

A new parameterisation for homogeneous ice nucleation driven by highly variable dynamical forcings

Alena Kosareva[1], Stamen Dolaptchiev[1], Peter Spichtinger[2], and Ulrich Achatz[1]

[1]Institut für Atmosphäre und Umwelt, Goethe-Universität Frankfurt, Frankfurt am Main, Germany
[2]Johannes Gutenberg-Universität Mainz, Mainz, Germany

Correspondence: Alena Kosareva (kosareva@iau.uni-frankfurt.de)

Abstract. The present work aims to extend the parameterisation of homogeneous ice nucleation introduced in Dolaptchiev et al. (2023) by incorporating variable ice mean mass and generalizing the approach under different conditions. The proposed method involves introducing an empirically derived correction based on a large data set of parcel model simulations. The method is validated against ensemble simulations using double-moment ice microphysics, showing a mean deviation of less than 16% from the reference solution, with robust performance across a range of conditions. The uncertainty of the extended parameterisation is evaluated for the increasing integration time steps. The method remains computationally efficient and produces sufficiently accurate results, even with larger time steps, making it suitable for integration into numerical weather prediction models. It is shown that the generalized approach not only provides a good representation of individual nucleation events but also effectively captures the statistics across the ensemble data. The prediction of ice mixing ratio is also assessed against the reference full double-moment system results. Despite a significant error in the initial prediction, it is demonstrated that the integration of the system over several time steps equilibrates the inconsistencies. This refined parameterisation offers a more accurate prediction of ice number concentration and ice mixing ratio and is not limited to gravity wave induced perturbations and can be supplemented by other relevant dynamical effects, such as turbulence.

1 Introduction

Cirrus clouds correspond to up to 30% of the total cloud cover, however they are still not well understood and their overall impact on climate in particular on the radiation forcing remains highly uncertain (e.g., Gasparini et al. (2018); Joos et al. (2014); Boucher et al. (2013)). The albedo effect and the greenhouse effect of these clouds are similar in magnitude, meaning the microphysical details such as number and shape of the ice crystals can significantly influence their net radiative effect (Krämer et al. (2020); Matus and L'Ecuyer (2017); Wang et al. (2020); Zhang et al. (1999)). Some studies also indicate the indirect effects of cirrus clouds on future climate (e.g. Gettelman et al. (2012)), which occurs mostly due to increases in ice crystal concentrations due to homogeneous nucleation from anthropogenic sulfur emissions.

These microphysical characteristics are affected by a complex interaction of the small-scale cloud processes and various interactions with the surrounding atmosphere. Observations suggest that gravity wave (GW) dynamics significantly impact the properties and life cycle of cirrus clouds (Kärcher and Ström (2003); Atlas and Bretherton (2023)).

https://doi.org/10.5194/gmd-2024-193
Preprint. Discussion started: 3 December 2024

Geoscientific Model Development Discussions

Vertical velocity perturbations, associated with gravity waves, turbulence or other processes, lead to the homogeneous freezing of aqueous solution droplets (Koop et al. (2000); Baumgartner et al. (2022)) at lower temperature conditions in the tropopause region. The effect of the gravity waves and other local dynamical processes on the nucleation has been widely investigated utilising different approaches for description of the updrafts. Those interactions are studied, for example in Dinh et al. (2016); Kärcher and Podglajen (2019) utilising a stochastic approach, in Joos et al. (2008) using a GW linear theory, and using the large-scale grid-resolved updraft velocity alongside with sub-grid-scale turbulence induced updrafts in Zhou et al. (2016).

Based on the results from Baumgartner and Spichtinger (2019) studying the homogeneous nucleation due to constant updraft velocities, Dolaptchiev et al. (2023) is extended the asymptotic approach to incorporate GW dynamics. The present work complements Dolaptchiev et al. (2023) and has been designed to further usage in connection with GW parameterisations for more realistic representation of GW-cirrus interactions. Recently transient and lateral-propagation effects have been introduced into GW parameterisations (Kim et al. (2021); Achatz et al. (2023); Voelker et al. (2024)). Corresponding parameterisations bear the potential to provide a more realistic representation of GW-cirrus interactions.

It was previously shown (Gierens et al. (2003)) that the deposition coefficient largely affects the nucleation process, while at the same time being dependent on the radius or mass of ice crystals. Mean mass variability have a significant effect on the cloud ice number concentration prediction, which is also observed in numerical parcel model simulations in Dolaptchiev et al. (2023). The influence of a cloud ice particle size uncertainty in a climate model was assessed in Wang et al. (2020)) and illustrates the sensitivity of the surface precipitation to the change in particle effective radius, due to the larger energy imbalance as well as spatial variability of short and long wave radiation. The effects of variable mass become more prominent in the conditions of higher number of pre-existing ice particles.

The current work focuses on generalizing the approach introduced in Dolaptchiev et al. (2023) to include mean mass variability for wide range of initial conditions. The asymptotic approach is supplemented by an empirical correction which can be used for various forcing representations. The proposed method is not restricted to the GW induced dynamics and can be used for large-scale updrafts or turbulent fluctuations. This work is also relevant for further implementation into a global numerical weather prediction (NWP) model, where it can be coupled to the dynamical parameterisations (e.g. GW and turbulence).

The article is organized as follows: The Sect. 2.1 provides a brief overview of the approach used and the motivation for its generalization. Sections 2.2 and 2.3 describe the chosen approach for constructing the parameterisation and technical details of the used data set. In the Sect. 3, the proposed parameterisation with corrections is verified against reference calculations, and the range of applicability is tested based on ensemble calculations. Concluding remarks can be found in Sect. 4.

2 Theory and methodology

2.1 Double-moment approach to ice physics representation coupled to GW

In the present work cirrus clouds are modeled using a double-moment bulk microphysics scheme (Spichtinger et al. (2023)) that assumes a unimodal ice mass distribution function, where first and second moments of the distribution function are ice mixing

https://doi.org/10.5194/gmd-2024-193
Preprint. Discussion started: 3 December 2024

Geoscientific Model Development Discussions
Open Access
EGU

ratio q_i and ice number concentration n_i. Ice crystals are assumed to have spherical shape, which simplifies the description of the properties. The scheme used here is described in Spichtinger and Gierens (2009); Spreitzer et al. (2017) with the addition of sedimentational sinks. The influence of Lagrangian pressure variations, e.g. due to GWs, on homogeneous nucleation and as well as mean mass variability are incorporated in Dolaptchiev et al. (2023). The resulting system of equations for n_i, q_i and saturation ratio over ice S reads:

$$\frac{Dn}{Dt} = J\exp(B(S-S_c)) + \frac{1}{\rho}\frac{\partial(\rho n v_n)}{\partial z}, \tag{1}$$

$$\frac{Dq}{Dt} = \frac{p_{si}}{p} D\left(\frac{q}{n}\right)^{1/3}(S-1)Tn + J\exp\Big(B(S-S_c)\Big) + \frac{1}{\rho}\frac{\partial(\rho q v_q)}{\partial z}, \tag{2}$$

$$\frac{DS}{Dt} = -D\left(\frac{q}{n}\right)^{1/3}(S-1)Tn - \frac{p}{p_{si}} J\exp\Big(B(S-S_c)\Big) - S\frac{1}{\pi}\frac{D\pi}{Dt}\left(\frac{L_i}{TR_v} - \frac{c_p}{R}\right). \tag{3}$$

Here saturation ratio is described as $S = \frac{p_v}{p_{si}}$, p_v is the water vapor pressure, p_{si} is the saturation pressure over ice, J is a homogeneous nucleation rate, B is a nucleation parameter, S_c is a critical saturation ratio, D is a deposition coefficient, v_n, v_q are sedimentation velocities, T is the temperature, ρ is the density, π is the Extner pressure. The values of used parameters are presented in Table A1. Equations (1)-(3) written in terms of material derivative $\frac{D}{Dt}$, i.e. all quantities are described following the motion of air parcels. Right hand parts of the system of equations describe the ice crystal growth due to the deposition of water vapor, the formation of new ice crystals through homogeneous nucleation and sedimentation of the ice crystals due to gravity. The later is not included into the consideration further because of the much larger sedimentation time scale (see Dolaptchiev et al. (2023)).

In Baumgartner and Spichtinger (2019) realistic air parcel simulations are conducted using a box model and a bulk microphysics scheme showing that for various environmental conditions assuming a constant mean mass is generally valid during long periods of the nucleation. However, just before nucleation, when the saturation ratio exceeds one, the ice crystals' mean mass increases, leading to a higher deposition rate. This increased deposition affects the saturation ratio over ice, which in turn influences the number of nucleated ice crystals. Given that it is crucial to include these effects in the current model, where the mean mass of ice crystals can be determined from the relation $m_{mean} = q_i/n_i$. This is achieved by incorporating the evolution equation for q_i and substituting $m(t) = q/n$ in the diffusional growth term.

Time scale separation is employed in Dolaptchiev et al. (2023) to assess the different processes and link the ice physics equations with the effects of GWs. The details of the coupling between the processes time scales and assumptions to the GW theory are presented in the Appendix.

Further study is done considering the ice physics of a single air parcel influenced by GW dynamics adopting a Lagrangian framework. In this case material derivatives in the system of equations are replaced by time derivatives $\frac{D}{Dt} = \frac{d}{dt}$.

https://doi.org/10.5194/gmd-2024-193
Preprint. Discussion started: 3 December 2024

Geoscientific Model Development Discussions
Open Access
EGU

As shown in Dolaptchiev et al. (2023), considering only dominant processes, the system of Eqs. (1)-(3) can be reduced to the following form:

$$\frac{dn}{dt} = J\exp(B(S-S_c)), \tag{4}$$

$$\frac{dq}{dt} = \frac{p}{p_{si}} D\left(\frac{q}{n}\right)^{1/3}(S-1)Tn, \tag{5}$$

$$\frac{dS}{dt} = -D\left(\frac{q}{n}\right)^{1/3}(S-1)Tn + SF(t). \tag{6}$$

Where $F(t)$ is a forcing term incorporating constant background updraft and GWs dynamics

$$F(t) = \frac{gL_i}{c_p R_v T^2}\left(w_{00} + \sum_j \hat{w}_j \cos(\omega_j t + \phi_j)\right).$$

Referring to the previous results from Dolaptchiev et al. (2023), in case of constant mass the asymptotic technique can be applied in order to obtain the prototype parameterisation. The nucleation event is determined where the saturation ration reaches the critical value S_c and the predicted value for the ice number concentration is found from:

$$N_{post} = \begin{cases} 2\frac{S_c F(t_0)}{D^{(*)}T(S_c-1)} - N_{pre}, & \text{if } N_{pre} < \frac{S_c F(t_0)}{D^{(*)}T(S_c-1)}; \\ N_{pre}, & \text{otherwise.} \end{cases} \tag{7}$$

Here $D^{(*)} = Dm_c^{1/3}$ is a deposition coefficient in case of constant mean mass with reference value $m_c = 10^{-12}$ kg, N_{pre}, N_{post} are the ice number concentrations before and after the nucleation event, t_0 is the time of a nucleation event when $S = S_c$.

In Dolaptchiev et al. (2023) the asymptotic approach was extended to account for the variable mass in the deposition coefficient, in the regime of slowly varying ice mixing ratio q_i during the nucleation event. In such a case the different processes can be decoupled and only n_i undergoes a quick change during the nucleation regime.

Numerical studies of the reduced system (4)-(6) based on a simplified parcel model showed several possible regimes relevant for the nucleation process (see Fig. 1). One regime under the conditions of high values of the pre-existing ice follows the same tendency as constant mass case. The evolution of parameters can be separated into three phases where the nucleation part is describing only the phase of rapid change of ice number concentration. Whereas the saturation ratio and ice mixing ratio change slowly during this short time and therefore can be assumed to not vary during this phase. However, conditions of low-to-zero pre-existing ice number concentrations lead to a different behaviour due to the deposition coefficient change. Assumptions of the time separation for the nucleation regime do not hold, since the ice mixing ratio is changing on the same time scale as ice number concentration. The extension to be proposed here aims to cover the whole range of initial conditions allowing to use the parameterisation accounting for mass variability independently from the regime.

2.2 Correction of the deposition coefficient for variable mean mass

In the present study we are utilising the previously obtained result for the constant mass case (7). This approach would allow for a clear physical relation between N_{post} and the initial number concentration and the forcing term at the point of the nucleation

https://doi.org/10.5194/gmd-2024-193
Preprint. Discussion started: 3 December 2024

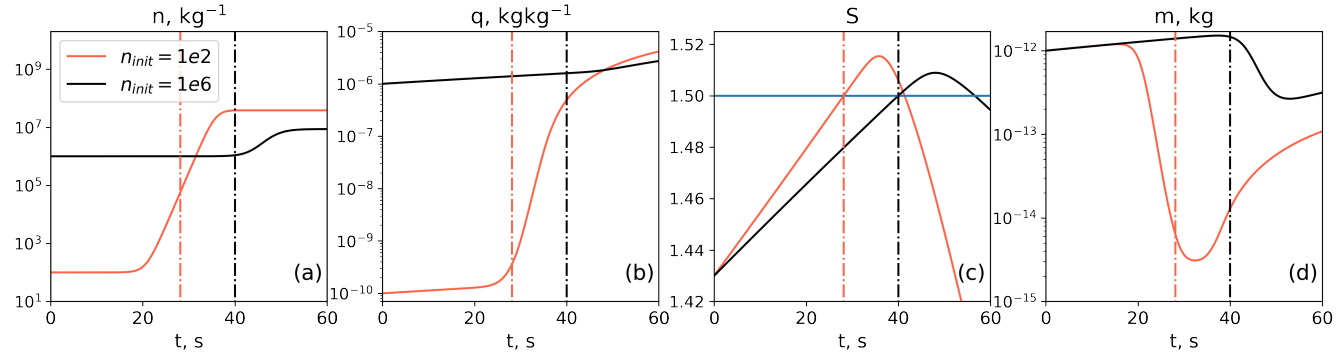

Figure 1. Evolution of the ice number concentration n, ice mixing ratio q, saturation ratio over ice S and mean mass of ice particles $m = q/n$ calculated based on system (4)-(6). Two cases of initial conditions: low pre-existing ice $n_{init} = 10^2$ kg^{-1} and higher values of pre-existing ice $n_{init} = 10^6$ kg^{-1}.

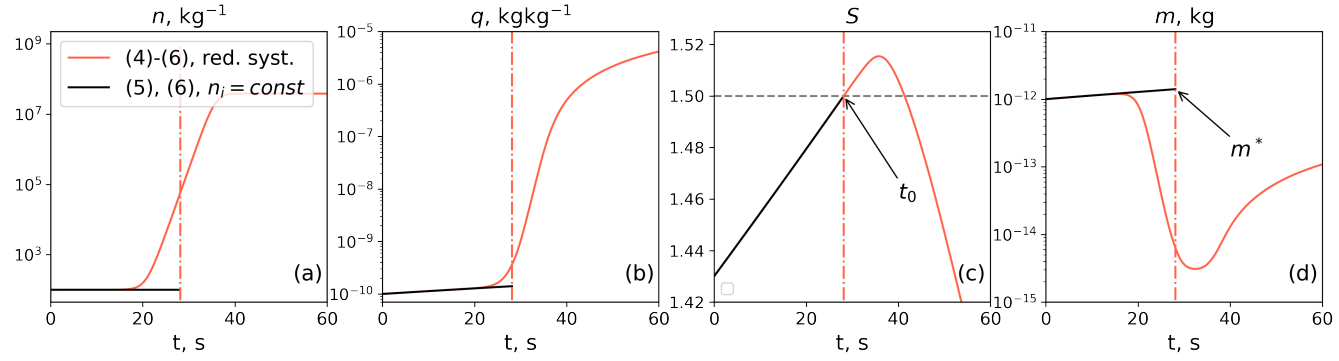

Figure 2. Evolution of the n, q, S, m in the reduced system (4)-(6) case and in the pre-nucleation regime, solving (5), (6) with assumption of $n = n_{init} = const$.

event. It would also account for different background conditions for temperature by design. Since mass variability changing the deposition coefficient directly, as one can see from (6), the straightforward solution is to correct the deposition coefficient in the constant mass parameterisation to a factor, representing the mass at the point of the nucleation event. The corrected parameterisation has the following form:

$$N_{post} = \begin{cases} 2\frac{S_c F(t_0)}{D^{(**)}(S_c-1)} - N_{pre}, & \text{if } N_{pre} < \frac{S_c F(t_0)}{D^{(**)}(S_c-1)}; \\ N_{pre}, & \text{otherwise}, \end{cases} \tag{8}$$

where $D^{(**)} = D\left(\frac{q_0}{n_0}\right)^{1/3}$ is a deposition coefficient corrected by a factor of $\left(\frac{q_0}{n_0}\right)$, t_0 is the time of the nucleation event and $q_0 = q(t_0)$, $n_0 = n(t_0)$.

https://doi.org/10.5194/gmd-2024-193
Preprint. Discussion started: 3 December 2024

Geoscientific Model Development Discussions

In order to find the the desired deposition coefficient one needs to define the parameters, which can be used for the correction. Figure 2 shows the evolution of the parameters calculated from the reduced system (4)-(6) and known pre-nucleation regime parameters, which can be used for deriving the correction and parameterisation. Here a pre-nucleation regime is defined as solution of the (4)-(6) system in the regime, where initial ice number concentration stays constant, which leads to solution of Eqs. (5),(6) with $n = n_{init} = const$ decoupled from Eq. 4. Sharp changes in the ice mixing ratio and mass in case of reduced system make it impossible to approximate the necessary q_0 or $\frac{q_0}{n_0}$ from pre-nucleation regime values itself. Therefore the correction to the deposition coefficient is approximated based on a large data set. Variables which can be used in the approximation include forcing term at the point of the nucleation event $F(t_0)$, initial number n_{init} and mass m^* predicted from the pre-nucleation regime, assuming no change in ice number concentration before the nucleation event.

The exact correction m_0 is determined from the results of the full system, such that the constant-mass approach leads to the observed N_{post}. Assuming a known evolution of the parameters during the nucleation event, Eq. (8), under the conditions allowing for further nucleation, can be solved for m_0:

$$m_0 = \left(\frac{2 S_c F(t_0)}{(N_{post} + N_{pre}) D (S_c - 1)} \right)^3, \tag{9}$$

where t_0, N_{pre}, N_{post} are known from the resolved full system (1)-(3).

Next we discuss the construction of the data set from the ensemble calculations based on (1)-(3) disregarding sedimentation process. The variability during the nucleation event depends on the initial conditions, such as ice number concentration, ice mixing ratio or mean mass of ice particles and on the gravity waves forcing. Since we want to represent the nucleation process itself the initial saturation ratio is set to a value of $S(t = 0) = 1.4$ close to the critical value. Other conditions are varied randomly using a uniform distribution in physically meaningful ranges motivated from the paper (Krämer et al. (2016)): we choose $10^{-4}\text{kg}^{-1} < n_{init}(t = 0) < 10^{7}$ kg^{-1}, and 10^{-16} kg $< m_{mean}(t = 0) < 10^{-12}$ kg.

Construction of the forcing is done based on the output from the global ICON model (Zängl et al. (2015)) coupled with GW parameterisation Multi-Scale Gravity Wave Model (MS-GWaM) (Bölöni et al. (2021); Kim et al. (2021); Achatz et al. (2023); Kim et al. (2023); Voelker et al. (2024)). This parameterisation is based on WKB theory (Bölöni et al. (2021)) and implemented using Lagrangian ray volumes, which are considered as carriers of the GW fields' wave-action density. The current version of the MS-GWaM allows to account for convectively generated GWs and GWs generated from processes other than convection or flow over mountains. Influence of the GWs generated by the mountains is incorporated by using original scheme (Lott and Miller (1997)) included in ICON model. For constructing the forcing term we utilize ICON version 2.6.5-nwp1, with 120 vertical levels and at horizontal resolution R2B5 (~ 80 km), the initial conditions are taken for 1st of May 2010 and the model integrated forward for 3 weeks, accounting for 2 weeks of spin-up. Information on subgrid-scale gravity wave related vertical wind perturbations is retrieved from MS-GWaM using the ray volume with maximum vertical wind amplitude per cell and corresponding frequency. In order to cover the variety of possible forcing term configurations the following cases are included in the data set construction:

1. Large-scale vertical velocity from ICON run w_{00}, in such a case the forcing term reads: $F(t) = \frac{g L_i}{c_p R_v T^2} w_{00}$;

https://doi.org/10.5194/gmd-2024-193
Preprint. Discussion started: 3 December 2024

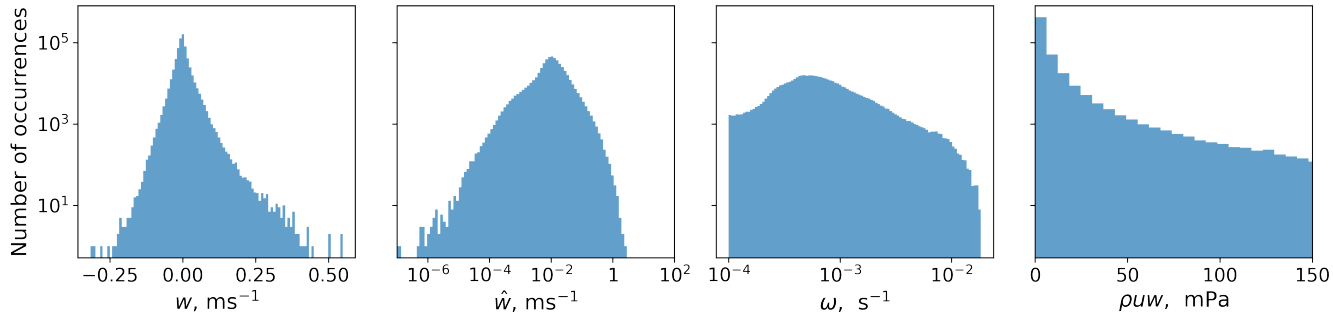

Figure 3. Number of occurrences of the large-scale vertical velocity w, vertical velocity amplitude $\hat{w}$, frequency of the GWs ω defined from the MS-GWaM parameterisation and momentum flux corresponding to the detected GW.

2. Single GW from MS-GWaM with maximum wind amplitude $\hat{w}$ within the cell, the corresponding frequency ω and phase ϕ which is picked randomly: $F(t) = \frac{gL_i\hat{w}}{c_pR_vT^2}\cos(\omega t + \phi)$;

3. Superposition of GWs, where the main GW is taken from MS-GWaM and other GWs have randomly varying amplitudes A_j, frequencies ω_j and phases ϕ_j independent from main GW and rescaled in the way, that the total momentum flux added is 1mPa: $F(t) = \frac{gL_i\hat{w}}{c_pR_vT^2}\cos(\omega t + \phi) + \sum_j \frac{gL_iA_j}{c_pR_vT^2}\cos(\omega_j t + \phi_j)$;

4. As in case 2 in the presence of background updraft w_{00}:
$F(t) = \frac{gL_i}{c_pR_vT^2}\Big(w_{00} + \hat{w}\cos(\omega t + \phi)\Big)$;

5. As in case 3 in the presence of background updraft w_{00}:
$F(t) = \frac{gL_i}{c_pR_vT^2}\Big(w_{00} + \hat{w}\cos(\omega t + \phi) + \sum_j \frac{gL_iA_j}{c_pR_vT^2}\cos(\omega_j t + \phi_j)\Big)$.

Distributions of the large scale vertical winds and vertical winds from the GWs used for constructing the forcing are presented on the Fig. 3. The probabilities for the corresponding frequency ω are also presented in Fig. 3 as well as those for the calculated GW momentum flux ρuw for the considered GW. The data is taken from the instantaneous output of global ICON simulation at the altitudes from 9 to 14 km, most relevant for cirrus formation. It is seen in Fig. 3 that large scale updraft is varied in range from -0.2 ms^{-1} up to 0.4 ms^{-1}, where in the majority of the cells vertical velocity is close to zero. Vertical wind perturbations $\hat{w}$ obtained from the GW parameterisation show stronger vertical velocity, with rare maximum above 1 ms^{-1}. Corresponding frequencies ω are sampled in a range between Coriolis parameter $f = 10^{-4}$ s^{-1} and buoyancy frequency $N = 2 \cdot 10^{-2}$ s^{-1} in the tropopause region and the form of the ω spectrum resembles the Desaubies form (Orr et al. (2010)). It is worth noting that resulting momentum flux based on the highest-amplitude ray volume is aligned with the observational statistics obtained from the balloon measurements (Hertzog et al. (2012)) and previously calculated momentum fluxes from the MS-GWaM parameterisation (Kim et al. (2021)). Therefore the total momentum flux considered lies in the physical range and the forcing term applied in the parcel simulations is not overestimated.

https://doi.org/10.5194/gmd-2024-193
Preprint. Discussion started: 3 December 2024

Geoscientific Model Development Discussions
Open Access
EGU

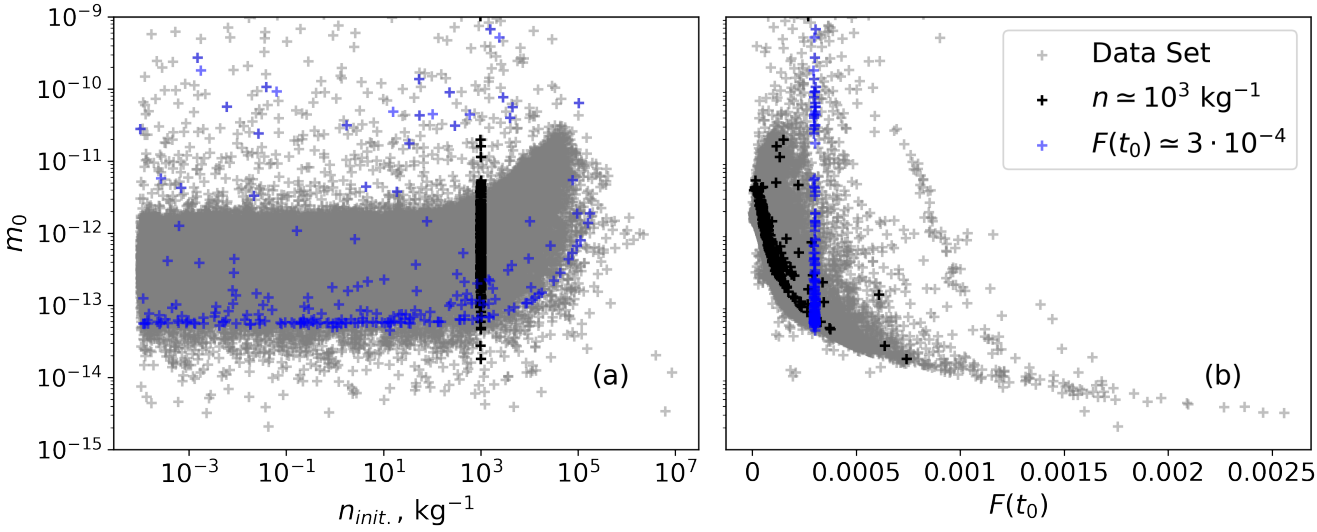

Figure 4. Exact m_0 correction depending on the initial number concentration (a) and on the forcing term value at the nucleation event point (b). Blue markers correspond to calculations with approximately same initial n_i, black markers correspond to calculation made with approximately same values of $F(t_0)$.

The exact correction m_0 is found from Eq. 9 based on the ensemble calculations for $\sim 2 \cdot 10^5$ nucleation events, the results are shown in Fig. 4. The data set is created using random initial conditions for n_i, q_i and various GW forcing configurations discussed above. The internal variability of the data is quite high, especially depending on the forcing term at the point of the nucleation event. However, by fixing certain parameters (blue and black markers) one can see the clear dependence of m_0 from the chosen parameters. Variability over forcing term is much larger, whereas under the conditions of smaller initial number concentrations m_0 stays nearly constant. The dependence on the forcing term is decaying with large variability for smaller values of the forcing at the point of the nucleation event.

2.3 Mean mass fitting for parameterisation

In the present section we consider options for approximating the dependence of m_0 based on the parameters known from the pre-nucleation regime. Since the ice mixing ratio q_i evolution is not captured in this regime (due to fixed deposition coefficient and n), one can fit the behaviour of the correction depending on the known parameters, such as initial ice number concentration n_{init} and forcing term at the point of the nucleation event $F(t_0)$.

Based on the created data set and relative behaviour of m_0 in dependence on n_{init} and $F(t_0)$, approximation to the data is found. The non-linear least squares method is applied to fit an assumed function to known data from ensemble simulations. The method requires to suggest a certain functional dependency on the parameters. Given the data set behaviour, the chosen

https://doi.org/10.5194/gmd-2024-193
Preprint. Discussion started: 3 December 2024

Geoscientific Model Development Discussions

simplified function is:

$$m_0(F(t_0), n_{init}) = \exp(a_1 + a_2 F(t_0)^{1/3} + a_3 n_{init}^{1/3} + a_4 n_{init} F(t_0)^{1/3}). \quad (10)$$

The mean error during the target data set reproduction is around 30% for set of $\sim 2 \cdot 10^5$ nucleation events with different GW forcing representations.

As an extension, a more complex dependency on n_{init}, $F(t_0)$, and involving one more parameter m^*, defined from pre-nucleation regime, is introduced and tested. The results showed improvement compared to the fit case. Mean error for ice number concentration prediction is reduced only by 2%. Besides, the advanced fit adds more complexity to the calculation, requires the use of an additional parameter and because of the additional terms used can lead to diverging results in cases out of sample range with regard to the reference data used for the parameter optimization.Therefore results presented below are obtained with the simplified fit approach only.

3 Results. Evaluation of the Model

Further results are shown for an independent data set consisting of 490 nucleation events, in order to validate the chosen fit. Initial conditions for n_i and m_i were created randomly, and the forcing term is based on ICON simulation different from the one used for the construction of the fit. In the following we will first asses the proposed fit. This will be followed bystability and accuracy tests depending on the time step chosen for the integration of the Eqs. (5)-(6) in the parameterised case.

3.1 Extended parameterisation

Comparison of the application of the chosen fit (10) and the exact mass calculated from the nucleation event simulations is shown in Fig. 5. Direct comparison of predictions with the exact values for m_0 shows a good agreement of the major part of the data points. Nonetheless the fit is not able to capture the higher possible m_0 values at higher initial n. Fig. 6 shows the exact post-nucleation ice number concentration and the one, obtained with the use of the extended parameterisation (8). The underestimation of the m_0 values at higher values of pre-existing ice leads to an overestimation of the ice number concentration as shown in Fig. 6.

Referring to the Fig. 5, the most frequently occurring cases of m_0 in the range between 10^{-13} kg and 10^{-12} kg, and the corresponding final N_{post} in Fig. 6, in the range between 10^5 and 10^6, are successfully represented by the chosen fit (10) and corrected parameterisation (8). However the outlying extreme cases are poorly captured due to simplicity of the fit. The overall behaviour of the fit stays similar to the exact data, therefore with decreasing n_{init} the prediction for the m_0 stays nearly independent from n_{init} (see Fig. 5). The cases with an increased forcing term correspond to the smaller values of m_0 increasing the final prediction for N_{post} in the exact data, and the same behaviour is captured by the fit.

To assess how well the chosen approach represents individual cases, the deviations of m_0 and N_{post} from their exact values are calculated. The probability density function (PDF) of the deviations is presented in Fig. 7. Here the deviations are calculated as $\Delta M = (M_{predicted} - M_{exact})/M_{exact} \cdot 100$ %, with $M = m_0, N_{post}$. The mean errors for m_0 and N_{post} predictions are 24%

https://doi.org/10.5194/gmd-2024-193
Preprint. Discussion started: 3 December 2024

Geoscientific Model Development Discussions

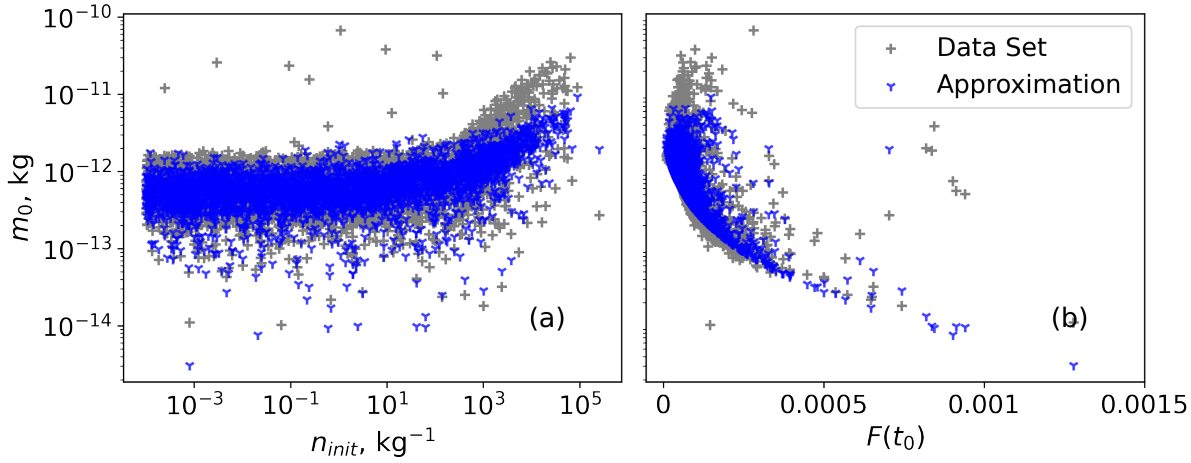

Figure 5. Exact m_0 correction depending on the initial number concentration and m_0 prediction from the constructed fit (10) for independent ensemble calculations.

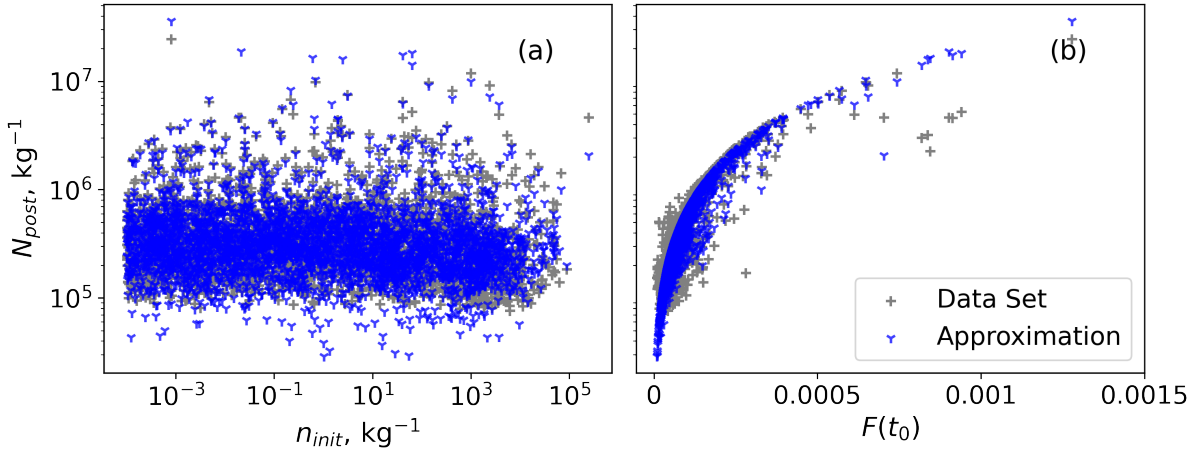

Figure 6. Post-nucleation ice number concentrations defined from the full system and prediction from the constructed parameterisation with correction (10).

and 16% correspondingly. More importantly, 90% of the error for prediction of the ice number concentration lies below 37%. Majority of the individual cases are represented sufficiently well, whereas outliers and poorly captured events with deviation in N_{post} above 50% correspond to less that 10% of the distribution.

For a better understanding of the prediction deviations we also consider PDF of the exact parameters and the approximated ones in order to asses the ability of our fit to capture the statistical properties of the data set. Previous ensemble simulations

https://doi.org/10.5194/gmd-2024-193
Preprint. Discussion started: 3 December 2024

Geoscientific Model Development Discussions

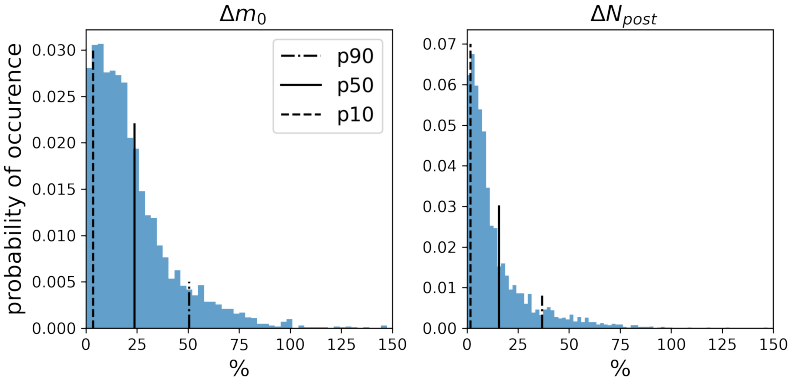

Figure 7. Probability density functions for deviations of the m_0 and N_{post} predictions from the exact solutions. Vertical lines correspond to 90th, 50th and 10th percentiles of the distribution.

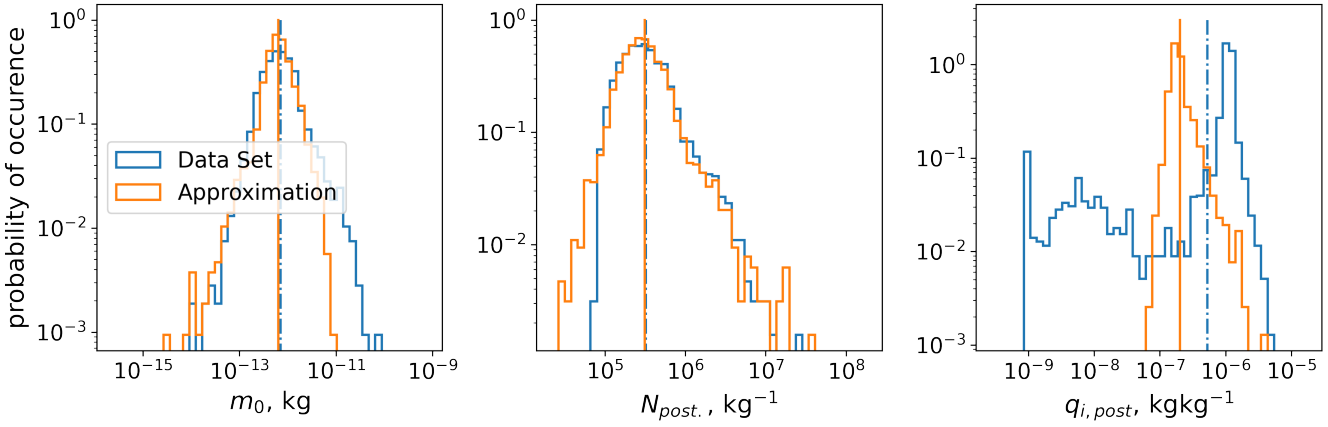

Figure 8. Probability density functions for m_0, N_{post} and q_i exact ensemble solutions and predictions. Vertical lines correspond to mean of the distribution.

using constant mass parameterisation (Dolaptchiev et al. (2023)) showed that while individual events can vary significantly, or even be missed, the statistical quantities for the ensemble still align well.

Comparisons of the PDFs for the mass m_0 correction, the predicted ice number concentration and the ice mixing ratio after the nucleation event are shown in Fig. 8. Here the prediction for the ice mixing ratio q_i is made based on the estimated mass m_0 and predicted by the corrected parameterisation ice number concentration N_{post} via $q_{i,post} = m_0 N_{post}$. Such approach contains some physical inconsistencies, because the approximated ice mean mass m_0 differs from the mean mass after the nucleation event, which is supposed to be used. However such estimation gives a suitable approximation for the further simulation of q_i. Further details are shown in Fig. 13 and 14 and discussed later in Sect. 3.2.

https://doi.org/10.5194/gmd-2024-193
Preprint. Discussion started: 3 December 2024

Geoscientific Model Development Discussions
Open Access
EGU

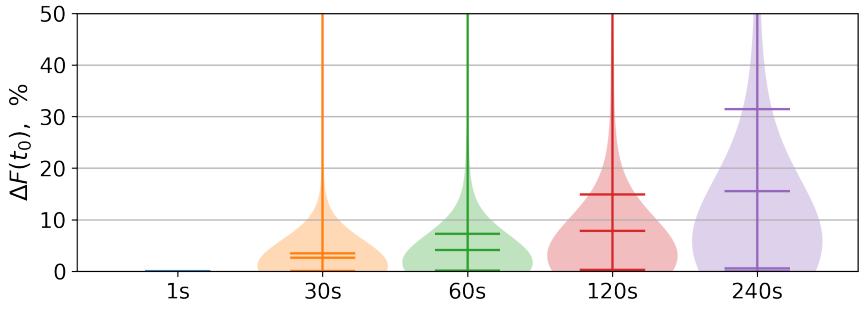

Figure 9. Probability density function of the deviation of detected from the parameterised approach $F(t_0)$ from the exact full system solution in %. Horizontal bars correspond to maximum, 90, 50, 10 percentiles and minimum of the distribution.

The PDF of the predicted mass from Fig. 8 at the point of the nucleation exhibits a slight underestimation of the mean value, due to the inability to correctly predict larger m_0 (also shown in Fig. 5). For the same reason the tail of the distribution is shorter and the maximum value has a mismatch of approximately one order of magnitude. The lower values of m_0 are represented better and the minimum values are in the same range. Comparison of the PDFs of the ice number concentration shows a good correspondence of major statistical indicators, such as mean, maximum and minimum values. However extended parameterisation gives occasional overestimation of N_{post} values for larger forcing term values and underestimation of the N_{post} in cases of small forcing (see right panel in Fig. 6). The comparison of ice mixing ratio PDFs can be considered as rough estimation of the q_i, which then is integrated over time with the larger time step. Therefore consistent underestimation of the q_i refers to a physical inconsistency discussed above. However, even with a roughly one order of magnitude underestimation, this prediction can still be used for further integration, minimizing the risk of numerical issues related to the rapid increase in q_i. Further the evolution of parameters for two isolated cases is presented on Figs. 13 and 14 to show the q_i prediction relevance.

3.2 Influence of the time step

The results shown in Sect. 3.1 are conducted using the same time step for the solution of the full system and coupled system (5),(6) employed in the parameterisation. Such decision is made in order to keep the results comparable without introducing further uncertainties. However, the major goal of the parameterisation is to increase the numerical performance especially by using larger time steps. Therefore, the following section is devoted to the depiction of the uncertainties and evaluation of the results under different used time steps.

The investigation of the stability of numerical integration and applicability of the defined approach is done based on a data set with 6 GWs and constant background updraft w_{00}. One of the sources of uncertainty is accuracy of the detection of the forcing term at the point of the nucleation where $S = S_c$. The nucleation event can be misplaced, changing the defined time of the nucleation event t_0, depending on the time step used for the calculation of the saturation ratio evolution (6). Calculation of the forcing term is sensitive to the changes in t_0, which leads to further errors in estimation of the $F(t_0)$ and other parameters.

https://doi.org/10.5194/gmd-2024-193
Preprint. Discussion started: 3 December 2024

Geoscientific Model Development Discussions

Further the deviations of the predictions from the exact values ΔM are calculated as mentioned before in Sect. 3.1 for the considered parameters $M = F(t_0), m_0, N_{post}$. First, in Fig. 9 we compare deviations in the forcing $F(t_0)$ when solving slow-scale processes for S, q_i based on system (5),(6) with five different time steps choices. The smallest chosen time step of one second gives the exact solution, whereas longer time steps lead to deviations from the exact prediction. Such deviations may influence the estimated m_0 via errors introduced in t_0 and $F(t_0)$ determination. However the crucial impact it would have on the N_{post} prediction by directly changing $F(t_0)$ in the formula (8). Maximum differences above 50% occur rarely and associated with outliers, for instance cases where nucleation event is missed with the usage of the larger time step. One of such cases is illustrated further in this section in Fig. 13. Mean deviations in the forcing term corresponding to the case of 30 seconds time step is 2.6%, and 90th percentile is 3.5%. The mean and the 90th percentile of the PDF are doubled with doubling the time step and rise up to 15% and 31% for the largest considered time step of two minutes. Considering the exact differences instead of relative errors it is found that larger time steps mostly lead to an underestimation of the forcing. Hence, because of the direct relation to the ice number concentration, one would expect underestimation of the N_{post} with increasing the time step.

Uncertainties from the detection of the forcing term then lead to a variation in m_0, considered in Fig. 10. The overall error we introduce by using the fit is illustrated by the first PDF when the same time step as in full system is used. Additional deviation introduced by differences in $F(t_0)$ leads to a variation of about 2-3% in the mean error of m_0, which is negligible compared to the overall error introduced by the fit.

Comparing the error of the ice number concentration prediction from the exact solution in Fig. 11, one observes the increase in the errors when going to higher time steps. The mean and 90th percentile of the distribution stay nearly the same when increasing the time step from 1 second to 60 seconds. The increase in mean error becomes larger for $dt = 120$ s and at $dt = 240$ s it becomes closer to 50%. We conclude that one can use a time step of 60 seconds without significant error increase. To estimate the quality of the new parameterisation, one can compare the mean errors to the relative accuracy of measurements (Krämer et al. (2016, 2020)). Mean error achieved with using time step of 60 seconds is of the same order as the accuracy of

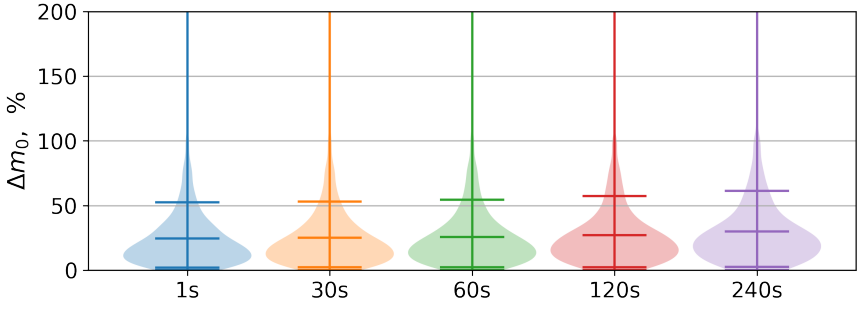

Figure 10. Probability density function of the deviation of m_0 predicted by fit (10) from exact mass calculated from the full system using (9) in %.

https://doi.org/10.5194/gmd-2024-193
Preprint. Discussion started: 3 December 2024

Geoscientific Model Development Discussions

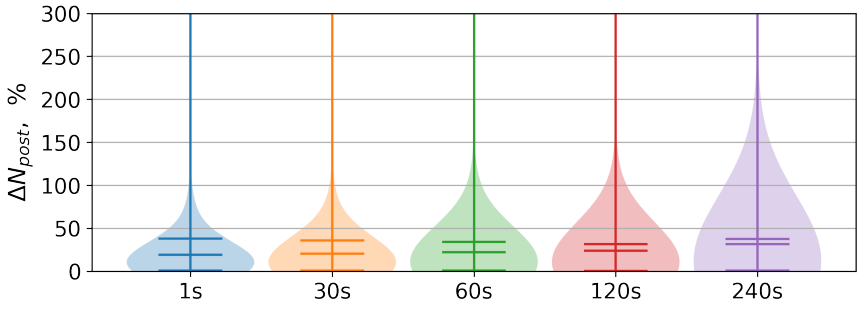

Figure 11. Probability density function of the deviation of N_{post} predicted using fit (10) by (8) from exact mass calculated from the full system in %.

measurements, which is about 20% (Luebke et al. (2016)). Therefore the proposed approach and chosen time step is sufficient for the representation of the process.

In order to check the dependence of the statistics on the time step used in integrating equations (5),(6), the comparison of the PDFs of m_0, N_{post} and q_i is shown in Fig. 12. The overall shape of approximated PDF of mass the m_0 agrees with the exact solution. However, the case with largest time step of two minutes shows underestimated m_0 minimum for several orders of magnitude. This leads to poor representation of the cases with higher N_{post} and consequent overestimation of the N_{post} maximum (see Fig. 12 middle panel). Predictions of the ice number concentrations are not far from the exact full system results if one compares the center of the PDF. The peak of the predicted N_{post} PDFs stays in the range of 2% difference compared to full system for all the parameterisation cases. However, the prediction made with using the largest time step considered substantially overestimates the maximum N_{post} value. It is worth to mention, that the ice number concentrations obtained with the parameterisation and full system are in the range of the observed quantities for the homogeneous nucleation (Krämer et al. (2020)).

Concerning the ice mixing ratio prediction, only the parameterisation with the finest time step gives underestimated q_i for the full PDF. The PDF of q_i is consistently increasing with increase of the time step, and peaks of the PDFs differ for about 50% for cases with time step of 30 and 60 seconds, and by the factor of 2 when using the 2 and 4 minutes time steps.

Further we present two nucleation events cases in order to directly compare the evolution and parameterisation prediction with different time step (see Figs. 13 and 14). By the means of such comparison one can make an additional conclusion on correctness and possibility of use of q_i as mentioned earlier and assess numerical stability of the method under different time steps. Initial conditions for presented cases are picked from the ensemble calculation with 6 superposed GWs with the presence of background updraft.

Both cases do not show any difference between the reduced system (4)-(6) and the full system (1)-(3). The corrected parameterisation (8) is tested for larger time step of 30, 120, 240 s, omitting the case with the smallest time step. The first case in Fig. 13 illustrates that parameterisation even with larger time steps gives a good agreement with the full system. The evolution of saturation ratio over ice, ice mixing ratio and mass are aligned with the full system results after some time following the

https://doi.org/10.5194/gmd-2024-193
Preprint. Discussion started: 3 December 2024

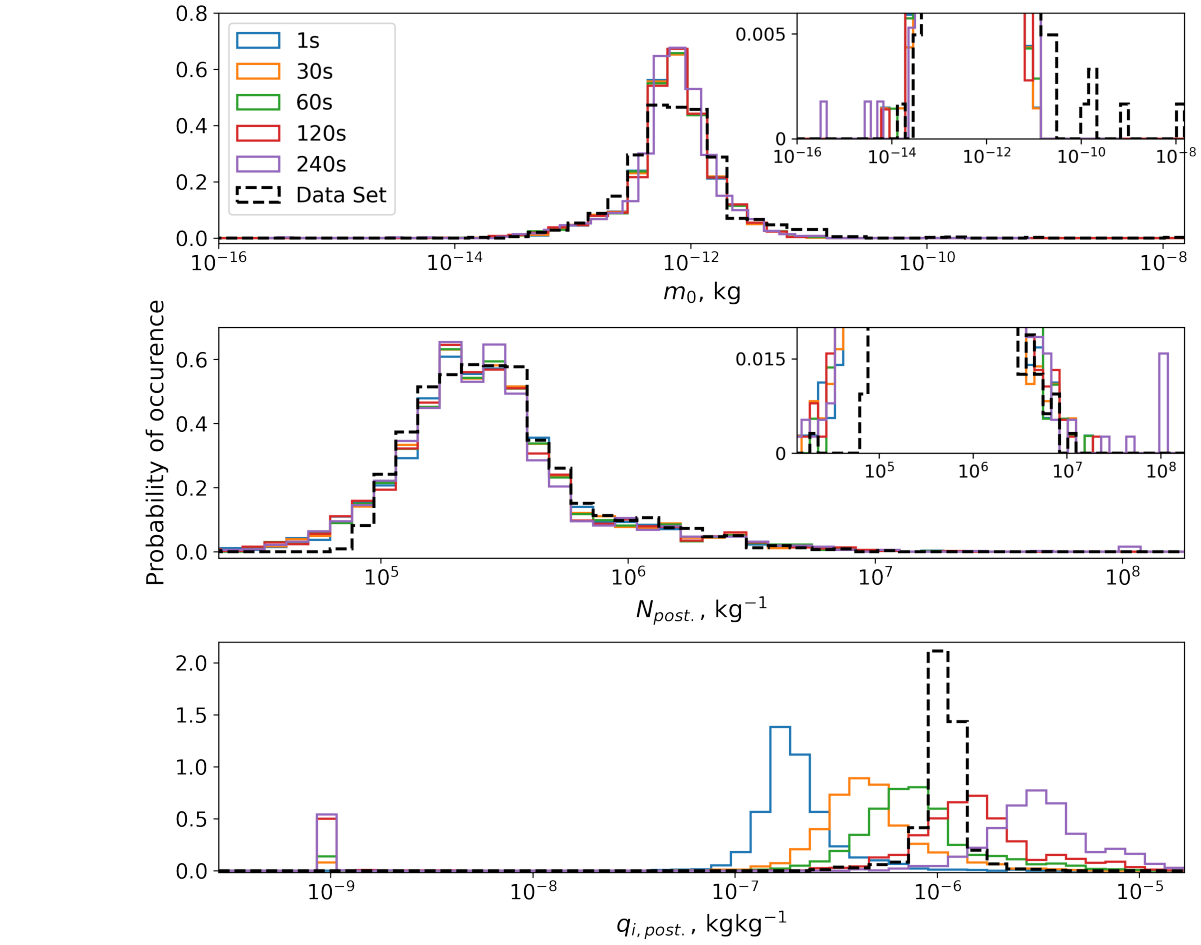

Figure 12. Probability density functions of m_0, N_{post} and q_i from the full model and predicted by the parameterisation (8) with different used time steps.

nucleation event. Prediction of the ice number concentration is not that exact for cases with larger time steps, but the difference is still in the range of 30%. After the prediction of q_i using the m_0 and N_{post} from the parameterisation one can see that integration is done without numerical problems. Evolution of ice mixing ratio shows a jump due to the nucleation process, followed by a short relaxation period, after which q_i prediction is adjusted and overlaps with the full system result.

The second test case presented in Fig. 14 has been picked on purpose to show several possible outcomes of using the parameterisation and consequences of usage of larger time steps. The evolution of the slowly-varying parameters such as S, q_i, m is captured relatively well by the parameterisation with the time steps of 30, 120 seconds. The largest considered time step, however, leads to smaller variations in the saturation ratio and hence the nucleation event is not captured by the parameterisation.

https://doi.org/10.5194/gmd-2024-193
Preprint. Discussion started: 3 December 2024

Geoscientific Model Development Discussions

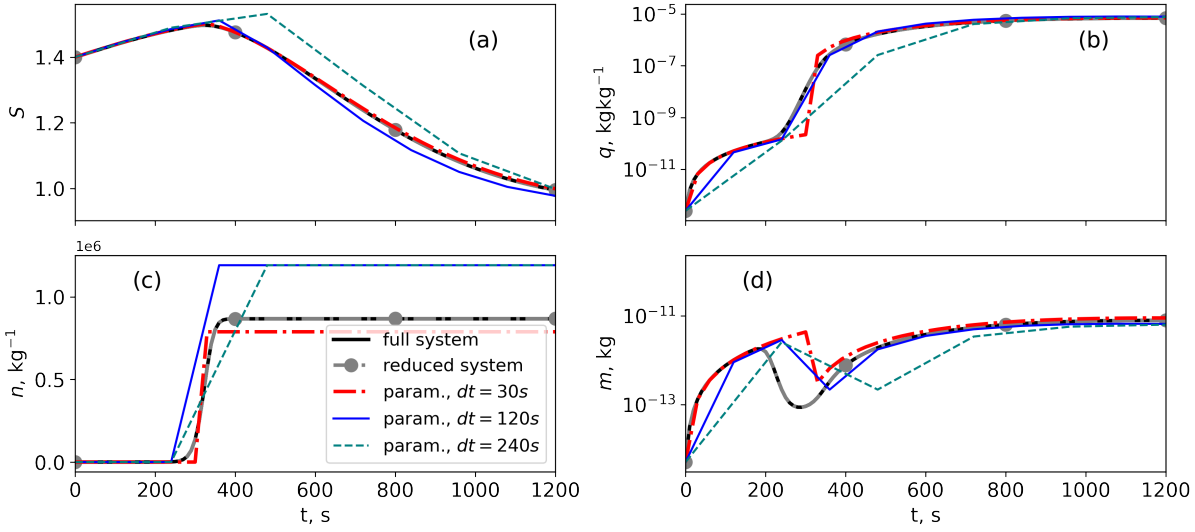

Figure 13. Comparison of the parameters evolution in full system, reduced system and parameterisation with proposed correction. Initial conditions: $S = 1.4$, $n = 50\ \mathrm{kg}^{-1}$, $q = 2.6 \cdot 10^{-13}\ \mathrm{kg\,kg}^{-1}$.

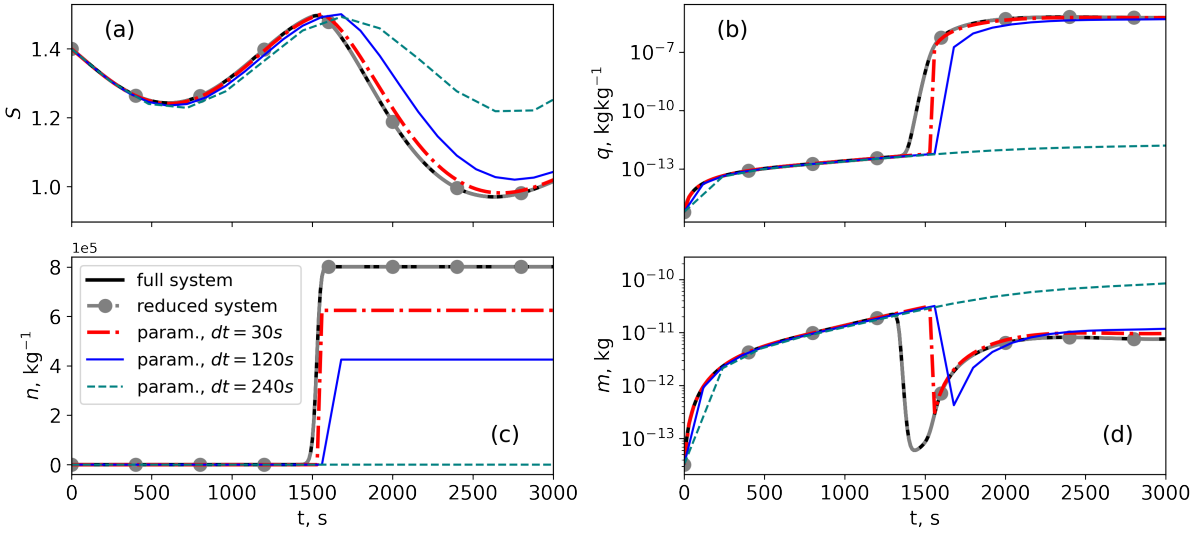

Figure 14. Comparison of the parameters evolution in full system, reduced system and parameterisation with proposed correction. Initial conditions: $S = 1.4$, $n = 0.018\ \mathrm{kg}^{-1}$, $q = 6 \cdot 10^{-16}\ \mathrm{kg\,kg}^{-1}$.

The parameterisation using a time step of 30 seconds gives a sufficiently good agreement with a deviation from the exact solution not larger than 22%. However, even though the parameterisation with 2 minutes time step predicts the nucleation event, the difference in the final ice number concentration is increased to 46%. Other variables and evolution of the slowly

https://doi.org/10.5194/gmd-2024-193
Preprint. Discussion started: 3 December 2024


Geoscientific Model Development Discussions
Open Access
EGU

varying part is described well in cases where the nucleation is captured as such. Considering different cases and referring to the representation of the PDFs the time step of 60 seconds can be suggested for parameterisation for the optimal result. Further increase in time step leads to the decrease of accuracy and in cases of a largest time step of 4 minutes even to a wrong representation of the process, where some events are not captured. Such behaviour is observed due to the fact that the pre-existing ice grows too fast, depleting the available water vapor and thus preventing the saturation ratio to increase to values triggering the nucleation.

4 Conclusions

A generalisation of the parameterisation derived in Dolaptchiev et al. (2023) including the effect of variable ice mean mass is proposed in the article. The employed approach has several advantages compared to constant mean mass assumption as the introduced correction to the deposition coefficient is dictated by the underlying physical difference in the deposition coefficient. The considered method allows to include the mean mass variation which leads to a better representation of the predicted ice number concentration distribution.

The new approach is validated against ensemble simulations based on the full double-moment scheme, showing a good agreement with the exact solution. The representation of individual nucleation events is sufficient and the mean deviation from the full system is less than 16% for the ice number concentration. A vast amount of cases is represented well, but the substantial differences remain for the extreme cases of the high forcing term values. The probability density function of the occurring n determined from independent ensemble simulations captures the major statistical characteristics such as mean and the center of the PDF.

Because of the computational efficiency demand for the NWPs application, the effect of uncertainties resulting from large microphysics time steps in the proposed extended parameterisation is assessed as well. The optimal representation of individual nucleation events combined with the sufficiently well captured statistics of N_{post} occurrence is achieved with the $dt = 60$ seconds. This recommendation is comparable with the fast physics time step of about 4 minutes used in large-scale NWP model. Evaluation of the numerical effectiveness shows that parameterisation is several times faster than solution of the full system with the time step of 1 second.

Further research involves implementation of the proposed approach for describing homogeneous ice nucleation in a global Numerical Weather Prediction (NWP) model. Besides the advanced description of the physical process by accounting for the mass variability, it is planned to employ an approach coupled to the dynamical parameterisations. The detailed representation of local subgrid-scale GWs dynamical fields impacting cirrus clouds is planned to be incorporated using the Multi-Scale Gravity Wave (MS-GWaM) parameterisation. Additionally, this approach can be supplemented by the other relevant dynamical effects, e.g. turbulence.

https://doi.org/10.5194/gmd-2024-193
Preprint. Discussion started: 3 December 2024

Geoscientific Model Development Discussions

Code and data availability. The air parcel model source code and Python scripts for processing and plotting the data are available on Zenodo at https://doi.org/10.5281/zenodo.14244119. Data set from ICON simulation used in the construction of the initial conditions for parcel model as well as all output data used for plots can be found on Zenodo at https://doi.org/10.5281/zenodo.13819511.

Appendix A

Coupling of the ice physics processes to the GW theory is done under the assumptions of mid-frequency and high-frequency GWs, where the GW time scale T_w is tied to the Brunt-Vaisala frequency $N = \sqrt{\frac{g}{\theta}\frac{d\bar{\theta}}{dz}}$ by the following relation:

$$T_w = \frac{1}{\varepsilon^\beta N}, \quad \beta = 0, 1; \quad \varepsilon = 0.1,$$

where $\beta = 0$ characterizes the high-frequency and $\beta = 1$ the mid-frequency GW time scale, ε is an introduced small parameter. For instance the characteristic time scales in the conditions of the troposphere, where $N = 10^{-2}$ s^{-1}, are $T_w = 100$ and $T_w = 1000$ seconds for the high and mid-frequency waves respectively. The diffusional growth time scale is estimated from $T_d = \left(Dm_c^{1/3}\frac{p_{si,c}}{p_{00}q_{v,c}}T_{00}n_c\right)^{-1}$ and has a value of about ~ 340 seconds. Here n_c is the reference ice number concentration, m_c is the reference mean mass of ice particles. Given the characteristic time scales and expanding the Exner pressure π in terms of a small parameter ε one can write the following expression for the derivative of π (Dolaptchiev et al. (2023)):

$$\frac{D\pi}{Dt} = \varepsilon^{2+\alpha}\frac{D\pi'}{Dt} + \varepsilon w\frac{d\bar{\pi}}{dz_s}, \tag{A1}$$

where $\pi = \left(\frac{p}{p_{00}}\right)^{\frac{R}{c_p}}$, $\alpha = 0$ corresponds to the strong and $\alpha = 1$ to the weak stratification case (Achatz et al. (2017, 2023)), $\bar{\pi}$ is the Extner pressure of the hydrostatically balanced reference atmosphere and π' describes the fluctuations due to the wave field.

As shown in Dolaptchiev et al. (2023), applying the scaling analysis one can neglect the first term on the right hand side in Eq. (A1). In case, where the leading order vertical velocity is solely due to a single GW, w in the second term of Eq. (A1) can be written as

$$w = |\hat{w}|^{(0)}\cos(\omega t_w + \phi).$$

For a superposition of j gravity waves, the following expression applies:

$$w = \sum_j |\hat{w_j}|\cos(\Omega_j t_w + \phi_j).$$

Here $\hat{w_j}$, Ω_j, ϕ_j are the vertical wind amplitude, frequency and phase of GW number j.

Substituting the following expressions in the Eq.(6) and also taking into account constant background updraft w_{00}, last term can be written in the following form:

$$F(t) = \frac{gL_i}{c_p R_v T_{00}^2}\Big(\sum_j \hat{w_j}\cos(\Omega_j t + \phi_j) + w_{00}\Big), \tag{A2}$$

where L_i is the latent heat of sublimation, g is the acceleration due to gravity, c_p is the heat capacity, R_v is the gas constant for dry air, T_{00} is the background reference temperature.

https://doi.org/10.5194/gmd-2024-193
Preprint. Discussion started: 3 December 2024

Geoscientific Model Development Discussions
Open Access
EGU

Table A1. Values or ranges for the physical quantities within the relevant ranges for UTLS region (Baumgartner and Spichtinger (2019); Dolaptchiev et al. (2023)).

Parameter	Description	Value or range
T_{00}	Reference background temperature	210 K
ρ_{00}	Reference background density	0.5 $\mathrm{kg\,m^{-3}}$
ρ_i	Ice particles density	920 $\mathrm{kg\,m^{-3}}$ to 929 $\mathrm{kg\,m^{-3}}$
p_{00}	Reference background pressure	300 hPa
J	Parameter for the nucleation rate	$4.9 \cdot 10^4$ $\mathrm{kg^{-1}s^{-1}}$
B	Parameter for the nucleation rate	337
S_c	Critical saturation ratio over ice	1.43 to 1.64
D	Deposition parameter	4.3 10^{-8} $\mathrm{kg^{2/3}s^{-1}K^{-1}}$
L_i	Latent heat of sublimation	$2.8 \cdot 10^6$ $\mathrm{Jkg^{-1}}$
c_p	Specific heat of dry air	1005 $\mathrm{J\,kg^{-1}K^{-1}}$
R	Gas constant for dry air	287 $\mathrm{J\,kg^{-1}K^{-1}}$
$p_{si,c}$	Reference saturation pressure over ice	1 Pa
n_c	characteristic ice number concentration	$2{\cdot}10^6$ $\mathrm{kg^{-1}}$
m_c	characteristic mean ice crystal mass	10^{-12} kg

Author contributions. AK and SD proposed the concept of generalization of the parameterisation. The extension was built based on the collaborative work of SD, PS, and UA, utilizing data produced from the ICON model with the gravity waves parameterisation developed within the group, under the leadership of UA. AK developed the methodology and conducted the investigation, defining the extended parameterisation with input from colleagues. The source code of the parcel model was developed by AK with assistance of SD, scripts for data analysis and outputs were written and documented by AK. Data interpretation was carried out collectively by all authors. AK wrote the manuscript, incorporating contributions and revisions from all co-authors. SD, UA, and PS provided supervision and guidance throughout the project.

Competing interests. The contact author has declared that none of the authors has any competing interests.

Acknowledgements. All authors thank the German Research Foundation (DFG) for support through the CRC 301 "TPChange" (Project-ID 428312742, Projects B06 “Impact of small-scale dynamics on UTLS transport and mixing”, B07 “Impact of cirrus clouds on tropopause structure”, and Z03 "Joint model development").

https://doi.org/10.5194/gmd-2024-193
Preprint. Discussion started: 3 December 2024

Geoscientific Model Development Discussions

References

Achatz, U., Ribstein, B., Senf, F., and Klein, R.: The interaction between synoptic-scale balanced flow and a finite-amplitude mesoscale wave field throughout all atmospheric layers: weak and moderately strong stratification, Quarterly Journal of the Royal Meteorological Society, 143, 342–361, 2017.

Achatz, U., Kim, Y.-H., and Voelker, G. S.: Multi-scale dynamics of the interaction between waves and mean flows: From nonlinear WKB theory to gravity-wave parameterizations in weather and climate models, Journal of Mathematical Physics, 64, 2023.

Atlas, R. and Bretherton, C. S.: Aircraft observations of gravity wave activity and turbulence in the tropical tropopause layer: prevalence, influence on cirrus clouds, and comparison with global storm-resolving models, Atmospheric Chemistry and Physics, 23, 4009–4030, 2023.

Baumgartner, M. and Spichtinger, P.: Homogeneous nucleation from an asymptotic point of view, Theoretical and Computational Fluid Dynamics, 33, 83–106, 2019.

Baumgartner, M., Rolf, C., Grooß, J.-U., Schneider, J., Schorr, T., Möhler, O., Spichtinger, P., and Krämer, M.: New investigations on homogeneous ice nucleation: the effects of water activity and water saturation formulations, Atmospheric Chemistry and Physics, 22, 65–91, 2022.

Bölöni, G., Kim, Y.-H., Borchert, S., and Achatz, U.: Toward transient subgrid-scale gravity wave representation in atmospheric models. Part I: Propagation model including nondissipative wave–mean-flow interactions, Journal of the Atmospheric Sciences, 78, 1317–1338, 2021.

Boucher, O., Randall, D., Artaxo, P., Bretherton, C., Feingold, G., Forster, P., Kerminen, V.-M., Kondo, Y., Liao, H., Lohmann, U., et al.: Clouds and aerosols, in: Climate change 2013: The physical science basis. Contribution of working group I to the fifth assessment report of the intergovernmental panel on climate change, pp. 571–657, Cambridge University Press, 2013.

Dinh, T., Podglajen, A., Hertzog, A., Legras, B., and Plougonven, R.: Effect of gravity wave temperature fluctuations on homogeneous ice nucleation in the tropical tropopause layer, Atmospheric Chemistry and Physics, 16, 35–46, 2016.

Dolaptchiev, S. I., Spichtinger, P., Baumgartner, M., and Achatz, U.: Interactions between Gravity Waves and Cirrus Clouds: Asymptotic Modeling of Wave-Induced Ice Nucleation, Journal of the Atmospheric Sciences, 80, 2861 – 2879, https://doi.org/https://doi.org/10.1175/JAS-D-22-0234.1, 2023.

Gasparini, B., Meyer, A., Neubauer, D., Münch, S., and Lohmann, U.: Cirrus cloud properties as seen by the CALIPSO satellite and ECHAM-HAM global climate model, Journal of Climate, 31, 1983–2003, 2018.

Gettelman, A., Liu, X., Barahona, D., Lohmann, U., and Chen, C.: Climate impacts of ice nucleation, Journal of geophysical research: Atmospheres, 117, 2012.

Gierens, K. M., Monier, M., and Gayet, J.-F.: The deposition coefficient and its role for cirrus clouds, Journal of Geophysical Research: Atmospheres, 108, 2003.

Hertzog, A., Alexander, M. J., and Plougonven, R.: On the intermittency of gravity wave momentum flux in the stratosphere, Journal of the Atmospheric Sciences, 69, 3433–3448, 2012.

Joos, H., Spichtinger, P., Lohmann, U., Gayet, J.-F., and Minikin, A.: Orographic cirrus in the global climate model ECHAM5, Journal of Geophysical Research: Atmospheres, 113, 2008.

Joos, H., Spichtinger, P., Reutter, P., and Fusina, F.: Influence of heterogeneous freezing on the microphysical and radiative properties of orographic cirrus clouds, Atmospheric Chemistry and Physics, 14, 6835–6852, 2014.

https://doi.org/10.5194/gmd-2024-193
Preprint. Discussion started: 3 December 2024

Kärcher, B. and Ström, J.: The roles of dynamical variability and aerosols in cirrus cloud formation, Atmospheric Chemistry and Physics, 3, 823–838, 2003.

Kim, Y.-H., Bölöni, G., Borchert, S., Chun, H.-Y., and Achatz, U.: Toward transient subgrid-scale gravity wave representation in atmospheric models. Part II: Wave intermittency simulated with convective sources, Journal of the Atmospheric Sciences, 78, 1339–1357, 2021.

Kim, Y.-H., Voelker, G. S., Bölöni, G., Zängl, G., and Achatz, U.: Crucial role of obliquely propagating gravity waves in the quasi-biennial oscillation dynamics, EGUsphere, 2023, 1–18, 2023.

Koop, T., Luo, B., Tsias, A., and Peter, T.: Water activity as the determinant for homogeneous ice nucleation in aqueous solutions, Nature, 406, 611–614, 2000.

Krämer, M., Rolf, C., Luebke, A., Afchine, A., Spelten, N., Costa, A., Meyer, J., Zoeger, M., Smith, J., Herman, R. L., et al.: A microphysics guide to cirrus clouds–Part 1: Cirrus types, Atmospheric Chemistry and Physics, 16, 3463–3483, 2016.

Krämer, M., Rolf, C., Spelten, N., Afchine, A., Fahey, D., Jensen, E., Khaykin, S., Kuhn, T., Lawson, P., Lykov, A., et al.: A microphysics guide to cirrus–Part 2: Climatologies of clouds and humidity from observations, Atmospheric Chemistry and Physics, 20, 12 569–12 608, 2020.

Kärcher, B. and Podglajen, A.: A Stochastic Representation of Temperature Fluctuations Induced by Mesoscale Gravity Waves, Journal of Geophysical Research: Atmospheres, 124, 11 506–11 529, https://doi.org/https://doi.org/10.1029/2019JD030680, 2019.

Lott, F. and Miller, M. J.: A new subgrid-scale orographic drag parametrization: Its formulation and testing, Quarterly Journal of the Royal Meteorological Society, 123, 101–127, 1997.

Luebke, A. E., Afchine, A., Costa, A., Grooß, J.-U., Meyer, J., Rolf, C., Spelten, N., Avallone, L. M., Baumgardner, D., and Krämer, M.: The origin of midlatitude ice clouds and the resulting influence on their microphysical properties, Atmospheric Chemistry and Physics, 16, 5793–5809, https://doi.org/10.5194/acp-16-5793-2016, 2016.

Matus, A. V. and L'Ecuyer, T. S.: The role of cloud phase in Earth's radiation budget, Journal of Geophysical Research: Atmospheres, 122, 2559–2578, 2017.

Orr, A., Bechtold, P., Scinocca, J., Ern, M., and Janiskova, M.: Improved middle atmosphere climate and forecasts in the ECMWF model through a nonorographic gravity wave drag parameterization, Journal of Climate, 23, 5905–5926, 2010.

Spichtinger, P. and Gierens, K. M.: Modelling of cirrus clouds–Part 1a: Model description and validation, Atmospheric Chemistry and Physics, 9, 685–706, 2009.

Spichtinger, P., Marschalik, P., and Baumgartner, M.: Impact of formulations of the homogeneous nucleation rate on ice nucleation events in cirrus, Atmospheric Chemistry and Physics, 23, 2035–2060, https://doi.org/10.5194/acp-23-2035-2023, 2023.

Spreitzer, E. J., Marschalik, M. P., and Spichtinger, P.: Subvisible cirrus clouds–a dynamical system approach, Nonlinear Processes in Geophysics, 24, 307–328, 2017.

Voelker, G. S., Bölöni, G., Kim, Y.-H., Zängl, G., and Achatz, U.: MS-GWaM: A 3-dimensional transient gravity wave parametrization for atmospheric models, Journal of the Atmospheric Sciences, 2024.

Wang, Y., Su, H., Jiang, J. H., Xu, F., and Yung, Y. L.: Impact of cloud ice particle size uncertainty in a climate model and implications for future satellite missions, Journal of Geophysical Research: Atmospheres, 125, e2019JD032 119, 2020.

Zängl, G., Reinert, D., Rípodas, P., and Baldauf, M.: The ICON (ICOsahedral Non-hydrostatic) modelling framework of DWD and MPI-M: Description of the non-hydrostatic dynamical core, Quarterly Journal of the Royal Meteorological Society, 141, 563–579, 2015.

Zhang, Y., Macke, A., and Albers, F.: Effect of crystal size spectrum and crystal shape on stratiform cirrus radiative forcing, Atmospheric Research, 52, 59–75, 1999.

https://doi.org/10.5194/gmd-2024-193
Preprint. Discussion started: 3 December 2024

Zhou, C., Penner, J. E., Lin, G., Liu, X., and Wang, M.: What controls the low ice number concentration in the upper troposphere?, Atmospheric Chemistry and Physics, 16, 12 411–12 424, https://doi.org/10.5194/acp-16-12411-2016, 2016.